

cis-9,10-Diethyl-9,10-dihydroanthracene (*cis*-6) was prepared by reductive alkylation of anthracene.¹⁹

trans-9,10-Diethyl-9,10-dihydroanthracene (*trans*-6) was prepared by Li/NH₃ reduction of 9,10-diethylanthracene.¹⁸

9,10-Ethano-9,10-dihydroanthracene (7) was prepared from dibenzobarrelene by Li/NH₃ reduction.²⁰

Benzanthrene (8) was prepared from commercial benzanthrone by reduction with a fourfold excess of LiAlH₄/AlCl₃.²¹

Ethylbenzanthrene (8a) was prepared from 8 (0.55 g, 2.5 mmol) by proton abstraction with *n*-butyllithium (3.1 mmol) in THF at -78 °C followed by the addition of excess bromoethane. Ether extraction yielded 8a as a yellow oil which was microdistilled for analysis. NMR (CCl₄) δ 0.5 (t, 3 H), 1.7 (quintet, 2), 4.1 (t, 1), 7.5 (m, 10).

Anal. Calcd for C₁₉H₁₆: C, 93.39; H, 6.61. Found: C, 93.66; H, 6.04. Mass spectrum, *m/e* 228.

trans-9-Ethyl-10-*tert*-butyl-9,10-dihydroanthracene (10) was prepared from 9-*tert*-butyl-9,10-dihydroanthracene by proton abstraction with *n*-butyllithium followed by alkylation with bromoethane.²²

(18) Harvey, R. G.; Arazadon, L.; Grant, J.; Urberg, K. *J. Am. Chem. Soc.* **1969**, *91*, 4535.

(19) Harvey, G. R.; Arazadon, L. *Tetrahedron* **1969**, *25*, 4887.

(20) Rabideau, P. W.; Jessup, D. W.; Ponder, J. W.; Beekman, G. F. *J. Org. Chem.* **1979**, *44*, 4594.

(21) See: Fieser, W.; Fieser, M. *Reagents for Organic Synthesis*; Wiley: New York, 1967; Vol. III, p 176.

cis-9-Ethyl-10-*tert*-butyl-9,10-dihydroanthracene (9) was prepared by epimerization of 10.²²

1,9-Ethano-9,10-dihydroanthracene (11) was prepared from aceanthrene²³ (230 mg, 1 mmol) and sodium (60 mg, 2.5 mmol) according to the general procedure for metal-ammonia reduction. After normal quenching with dilute ammonium chloride solution and ether extraction, the solid product was recrystallized from methanol/water to yield 1,9-ethano-9,10-dihydroanthracene as white crystals: mp 81-82 °C (60 mg, 0.3 mmol, 33%); NMR (CDCl₃) δ 2.0 (m, 1 H), 2.9 and 3.1 (m, 3), 3.8 (m, 3), 7.1 (br d, 7).

Anal. Calcd for C₁₆H₁₄: C, 93.15; H, 6.85. Found: C, 93.36; H, 6.60.

Acknowledgment. We gratefully acknowledge support from the U.S. Department of Energy, Office of Basic Energy Science, and the Indiana University Computer Network.

(22) Fu, P. P.; Harvey, R. G.; Paschal, J. W.; Rabideau, P. W. *J. Am. Chem. Soc.* **1975**, *97*, 1145.

(23) Aceanthrene was prepared starting from aceanthrenequinone according to the synthesis reported by Becker et al. (Becker, H. D.; Hansen, L.; Naderson, K. *J. Org. Chem.* **1985**, *50*, 277) with one exception. 2-Aceanthrone was prepared with pyridine hydrochloride reagent as described by Plummer et al. (Plummer, B. F.; Al-Saigh, Z. Y.; Arfan, M. *J. Org. Chem.* **1984**, *49*, 2069). Melting points of intermediate compounds were identical with those reported by Becker et al.

The Complexation of Sodium Ion by the Cryptand 4,7,13-Trioxa-1,10-diazabicyclo[8.5.5]eicosane (C21C₅) in a Range of Solvents. A ²³Na Nuclear Magnetic Resonance Kinetic Study

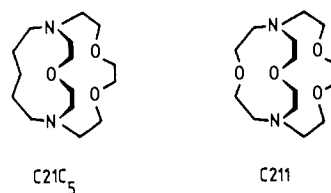
Stephen F. Lincoln,*[†] Ian M. Brereton,[‡] and Thomas M. Spotswood[‡]

Contribution from the Department of Physical and Inorganic Chemistry, and the Department of Organic Chemistry, University of Adelaide, Adelaide, South Australia 5001, Australia.
Received March 24, 1986

Abstract: The exchange of Na⁺ between the solvated state and the cryptate [Na·C21C₅]⁺ has been studied in acetonitrile, propylene carbonate, acetone, methanol, dimethylformamide, and pyridine solvents by ²³Na NMR spectroscopy. The decomplexation rate constants *k_d*(298.2 K) = 19.4 ± 0.5 and (2.88 ± 0.03) × 10⁴ s⁻¹ determined in propylene carbonate and dimethylformamide, respectively, encompass the variation of lability toward decomplexation exhibited by [Na·C21C₅]⁺ in the six solvents studied. The [Na·C21C₅]⁺ formation rate constants 10⁻⁵*k_f*(298.2 K) = 4.9 and 214 dm³ mol⁻¹ s⁻¹ determined in pyridine and dimethylformamide, respectively, encompass the much smaller variation of the lability of the formation process and demonstrate that the variation of *k_d* dominates the variation of the stability of the cryptate with the nature of the solvent. By comparison *k_d* for [Na·C211]⁺ is 500-2000 times less than that for [Na·C21C₅]⁺, and the greater lability toward decomplexation of the latter cryptate is attributed to C21C₅ possessing only three oxygen donor atoms whereas C211 has four such atoms. However, *k_f* for [Na·C211]⁺ is smaller than *k_f* for [Na·C21C₅]⁺ by a factor of 10 or less. These observations and the dependence of *k_f* and *k_d* on the nature of the solvent are used to postulate reaction mechanisms for the two cryptates.

Since the introduction of the polyoxadiazabicycloalkane or cryptand ligands by Lehn the solution chemistry of the complexes, or cryptates, formed between alkali metal ions and cryptands has been the subject of extensive study.¹⁻¹² Investigations of the effect of metal ion size and cryptand cavity size on stability and lability have produced a substantial understanding of the mechanism of cryptate formation,^{5-8,10} but there is a relative paucity of systematic data on the effect of the cryptand donor atoms on these characteristics. This study seeks insight into this aspect of the cryptates through a kinetic investigation of Na⁺ exchange on the cryptate formed by 4,7,13-trioxa-1,10-diazabicyclo[8.5.5]eicosane (C21C₅) in a range of solvents and a comparison of the derived kinetic

Chart I



parameters with those characterizing the closely related 4,7,13,18-tetraoxa-1,10-diazabicyclo[8.5.5]eicosane (C211) sys-

* Department of Physical and Inorganic Chemistry.

† Department of Organic Chemistry.

(1) Lehn, J.-M. *Struct. Bonding (Berlin)* **1973**, *16*, 1-69.

(2) Lehn, J.-M.; Sauvage, J. P. *J. Am. Chem. Soc.* **1975**, *97*, 6700-6707.

Table I. Solution Compositions and ^{23}Na Chemical Shifts^a (261.5 K) for the $[\text{Na}\cdot\text{C21C}_5]^+$ System

soln	solvent	$[\text{NaClO}_4]$ mol dm ⁻³	$[\text{C21C}_5]$ (tot.) mol dm ⁻³	δ (Na ⁺ solvated) ppm	δ ($[\text{Na}\cdot\text{C21C}_5]^+$) ppm
i	acetonitrile	0.105	0.053	2.30	11.95
ii	acetonitrile	0.105	0.070	2.37	11.83
iii	propylene carbonate	0.101	0.050	-4.57	12.14
iv	propylene carbonate	0.101	0.068	-4.51	12.05
v	acetone	0.102	0.051	-2.22	10.60
vi	acetone	0.102	0.068	-2.15	10.73
vii	methanol	0.099	0.049	1.68	12.57
viii	methanol	0.099	0.066	1.64	12.41
ix	dimethylformamide	0.106	0.053	0.00	9.20 ^b
x	dimethylformamide	0.106	0.071	0.10	9.10 ^b
xi	pyridine	0.106	0.053	5.05	12.90
xii	pyridine	0.106	0.073	4.92	12.79

^aChemical shifts referenced to 0.100 mol dm⁻³ NaClO₄ in dimethylformamide at 261.5 K. ^bExtrapolated from spectra at lower temperatures as this system exhibits chemical exchange induced line broadening at 261.5 K. The digital resolution of all spectra was 0.03 ppm.

tem.^{8,10} (It is seen from Chart I that C21C₅ differs from C211 only by the replacement of an oxygen by a methylene group.) In the solid state $[\text{Na}\cdot\text{C21C}_5]^+$ and $[\text{Na}\cdot\text{C211}]^+$ exist as exclusive cryptates in which Na⁺ resides above the 15-membered ring of C21C₅ delineated by two nitrogens and three oxygens¹¹ (in contrast to inclusive $[\text{Li}\cdot\text{C21C}_5]^+$ and $[\text{Li}\cdot\text{C211}]^+$ where Li⁺ resides in the cryptand cavities^{13,14}), and ¹³C NMR studies indicate that these exclusive structures are largely retained in solution.⁹⁻¹¹ The apparent stability constant, *K*, of $[\text{Na}\cdot\text{C21C}_5]^+$ varies substantially with the nature of the solvent as shown by the log (*K*/dm³ mol⁻¹) = 2.87, 3.72, 3.76, 3.98, 5.08, and 5.12 values determined at 298.2 K in dimethylformamide, pyridine, methanol, acetone, acetonitrile, and propylene carbonate, respectively,¹² which are substantially lower than those determined for $[\text{Na}\cdot\text{C211}]^+$.⁷ It is a prime objective of this study to determine the kinetic and mechanistic origins of these differences in stability arising from both the replacement of an oxygen in C211 by a methylene group to give C21C₅ and from the variation in the nature of the solvent.

Experimental Section

The cryptand C21C₅ was prepared as previously described.¹¹ Sodium perchlorate (Fluka) was dried at 353–363 K under vacuum for 48 h and was stored over P₂O₅ under vacuum. Acetonitrile, propylene carbonate, acetone, methanol, dimethylformamide, and pyridine were purified and dried as described in the literature¹⁵ and were stored over Linde 3-Å molecular sieves under nitrogen. The water content of these solutions was below the Karl-Fischer detection level of ca. 50 ppm.

Solutions of NaClO₄ and C21C₅ were prepared under dry nitrogen and were sealed under vacuum in 5-mm NMR tubes which were coaxially inserted into 10-mm NMR tubes containing either D₂O, acetone-*d*₆ or dimethyl sulfoxide-*d*₆ which acted as lock solvents. The concentrations of the solutions appear in Table I.

²³Na NMR spectra were run on either Bruker CXP-300 or HX-90E spectrometers operating at 79.39 and 23.81 MHz, respectively, depending on the magnitude of the chemical shift difference (Table I) between the resonances of solvated Na⁺ and $[\text{Na}\cdot\text{C21C}_5]^+$, and the temperature range

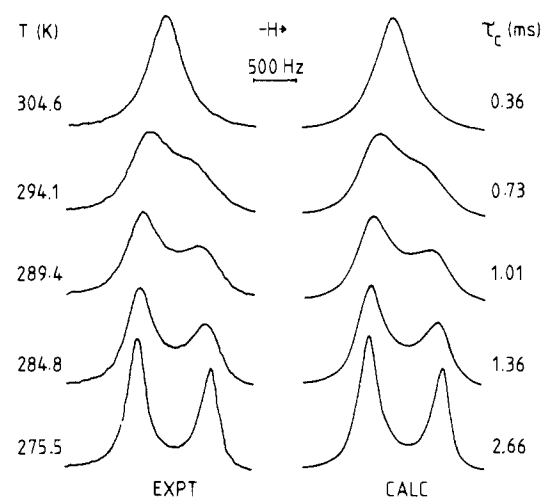


Figure 1. Typical exchange modified 79.39-MHz ^{23}Na NMR spectra of a methanol solution of NaClO₄ (0.099 mol dm⁻³) and C21C₅ (0.066 mol dm⁻³). Experimental temperatures and spectra appear at the left of the figure, and best fit calculated line shapes and corresponding τ_c values appear at the right of the figure. The resonance of $[\text{Na}\cdot\text{C21C}_5]^+$ appears downfield from the resonance of solvated Na⁺.

Table II. Selected Distances from the Crystal Structures^a of the Cryptates $[\text{Na}\cdot\text{C21C}_5\cdot\text{NCS}]^+$ and $[\text{Na}\cdot\text{C211}\cdot\text{NCS}]^+$

distance ^b Å	cryptate	
	$[\text{Na}\cdot\text{C21C}_5\cdot\text{NCS}]^+$	$[\text{Na}\cdot\text{C211}\cdot\text{NCS}]^+$
Na-O(1)	2.297 (2)	2.289 (14)
Na-O(2)	2.340 (3)	2.324 (13)
Na-O(3)	2.356 (2)	2.433 (19)
Na-O(4)		2.662 (9)
Na-N(1)	2.759 (4)	2.478 (13)
Na-N(2)	2.576 (3)	2.492 (17)
Na-NCS	2.358 (4)	2.409 (11)
Na-O ₃ plane	0.37	0.14

^aData from ref 11. ^bThe atomic numbering runs in the sequence N(1), O(1), N(2), O(2), O(3) around the N₂O₃ ring to which Na⁺ is bound.

in which the site exchange induced coalescence of these resonances was observed. Thus the exchange process was too slow to produce coalescence in the liquid temperature range of acetonitrile at 79.39 MHz, but at 23.81 MHz the coalescence was observed in this temperature range. Coalescence was conveniently observed at 79.39 MHz for the other five solvents as seen for methanol in Figure 1. For each solution an average of 6000 transients was accumulated in a 2048 point data base at temperature intervals of ca. 5 K. Sample temperature was controlled by Bruker B-VT1000 variable temperature units to within ± 0.3 K. The Fourier transformed spectra were subjected to complete line shape analysis¹⁶ on a Nicolet BNC12 minicomputer. The ²³Na line widths and chemical shifts (and their temperature dependences) employed in the line shape

- (3) Lehn, J.-M. *Acc. Chem. Res.* **1978**, *11*, 49–57.
 (4) Cahen, Y. M.; Dye, J. L.; Popov, A. I. *J. Phys. Chem.* **1975**, *79*, 1289–1291.
 (5) Cahen, Y. M.; Dye, J. L.; Popov, A. I. *J. Phys. Chem.* **1975**, *79*, 1292–1295.
 (6) Popov, A. I. *Pure Appl. Chem.* **1979**, *51*, 101–110.
 (7) Cox, B. G.; Garcia-Rosa, J.; Schneider, H. *J. Am. Chem. Soc.* **1981**, *103*, 1054–1059.
 (8) Cox, B. G.; Garcia-Rosa, J.; Schneider, H. *J. Am. Chem. Soc.* **1981**, *103*, 1384–1389.
 (9) Schmidt, E.; Tremillon, J.-M.; Kintzinger, J.-P.; Popov, A. I. *J. Am. Chem. Soc.* **1983**, *105*, 7563–7566.
 (10) Lincoln, S. F.; Brereton, I. M.; Spotswood, T. M. *J. Chem. Soc., Faraday Trans. 1* **1985**, *81*, 1623–1630; **1986**, *82*, 1999.
 (11) Lincoln, S. F.; Horn, E.; Snow, M. R.; Hambley, T. W.; Brereton, I. M.; Spotswood, T. M. *J. Chem. Soc., Dalton Trans.* **1986**, 1075–1080.
 (12) Lincoln, S. F.; Steel, B. J.; Brereton, I. M.; Spotswood, T. M. *Polyhedron*, in press.
 (13) Abou-Hamdan, A.; Hambley, T. W.; Hounslow, A. M.; Lincoln, S. F. *J. Chem. Soc., Dalton Trans.*, in press.
 (14) Moras, D.; Weiss, R. *Acta Crystallogr., Sect. B: Struct. Crystallogr. Cryst. Chem.* **1973**, *B29*, 400–403.
 (15) Perrin, D. D.; Aramaego, W. L. F.; Perrin, D. R. *Purification of Laboratory Chemicals*, 2nd ed.; Pergamon: Oxford, 1980.

(16) Lincoln, S. F. *Prog. React. Kinetics* **1977**, *9*, 1–91.

Table III. Kinetic Parameters^a for Na⁺ Exchange on [Na·C21C₅]⁺ and [Na·C211]⁺ in Various Solvents

solvent	D _N ^b	cryptand	10 ⁻⁵ k _f (298.2 K) ^c dm ³ mol ⁻¹ s ⁻¹	k _d (298.2 K) s ⁻¹	ΔH _d ⁺ kJ mol ⁻¹	ΔS _d ⁺ J K ⁻¹ mol ⁻¹
acetonitrile	14.1	C21C ₅	100	84.8 ± 1.6	57.9 ± 0.7	-13.8 ± 2.1
propylene carbonate	15.1	C21C ₅	25.5	19.4 ± 0.5	70.3 ± 0.5	15.3 ± 1.4
acetone	17.0	C21C ₅	84	878 ± 6	54.4 ± 0.4	-6.1 ± 1.2
methanol	19.0	C21C ₅	104	1800 ± 50	44.9 ± 0.1	-31.9 ± 0.4
dimethylformamide	26.6	C21C ₅	214	28800 ± 300	40.0 ± 0.1	-25.3 ± 0.5
dimethyl sulfoxide	29.8	C21C ₅		large		
pyridine	33.1	C21C ₅	4.9	93.5 ± 0.5	62.8 ± 0.2	3.3 ± 0.5
propylene carbonate ^d	15.1	C211	210	0.036		
water ^e	18.1	C211	0.754	47.6 ± 0.5	67.2 ± 0.3	12.6 ± 0.7
methanol ^d	19.0	C211	31.0	2.5		
dimethylformamide ^e	26.6	C211	19.2	12.1 ± 0.2	83.5 ± 0.5	55.8 ± 1.2
dimethyl sulfoxide ^e	29.8	C211	14.5	34.0 ± 0.7	69.5 ± 0.4	17.4 ± 1.2
methanol ^d	19.0	C221	1700	0.023		
dimethylformamide ^d	26.6	C221	180	0.75		

^a Quoted errors represent one standard deviation obtained from a linear regression analysis of the temperature dependence of experimental τ_c data through eq 2. ^b Gutmann donor number from ref 18. The dielectric constants from the same reference are as follows: acetonitrile, 38.0; propylene carbonate, 69.0; acetone, 20.7; methanol, 32.6; dimethylformamide, 36.1; dimethyl sulfoxide, 45.0; and pyridine, 12.3. (It should be noted that other authors have used D_N values for some solvents which differ from those originally derived by Gutmann—e.g., Strasser, B. O.; Popov, A. I. *J. Am. Chem. Soc.* 1985, 107, 7921–7924. ^c $k_f = k_d K$ where $\log (K/\text{dm}^3 \text{mol}^{-1}) = 5.08, 5.12, 3.98, 3.76, 2.87,$ and 3.72 in acetonitrile, propylene carbonate, acetone, methanol, dimethylformamide, and pyridine, respectively, at 298.2 K, and they are taken from ref 12. ^d Reference 8. ^e Reference 10.

analysis were obtained through a combination of extrapolation from low temperature where no exchange induced modification occurred, and the determination of ²³Na line widths and shifts in solutions containing either solvated Na⁺ or [Na·C21C₅]⁺ alone in the coalescence temperature range observed for the solutions which contained both species.

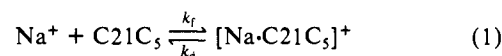
Results and Discussion

As mechanistic arguments presented here depend to a significant extent on a knowledge of cryptate structure it is appropriate to briefly review the structural data for the cryptates of interest before considering the kinetic data. Crystalline [Na·C21C₅·NCS] and [Na·C211·NCS] exist as exclusive cryptates in which Na⁺ is sited above the 15-membered ring delineated by the two nitrogen and three oxygen atoms of C21C₅ and C211 (hereafter called the N₂O₃ ring), and the nitrogen of NCS⁻ is also within bonding distance of Na⁺ but on the side opposite the N₂O₃ ring.¹¹ The existence of both cryptates in the exclusive form is not surprising as Na⁺ (which has a six-coordinate ionic radius¹⁷ of 1.02 Å) appears to be too large to fit into the C21C₅ and C211 cavities which have diameters of ca. 1.6 Å.² There are, however, significant structural differences between the two cryptates as is seen from the selected bond distances presented in Table II. It is seen that the Na⁺ distances to the O(1) and O(2) atoms of the N₂O₃ ring are indistinguishable in the two cryptates, whereas the Na–N distances and the distance of Na⁺ above the plane of the three oxygens of the N₂O₃ ring (O₃ plane) are significantly greater in [Na·C21C₅·NCS]. These differences are probably a consequence of the interaction between Na⁺ and the fourth oxygen (which are only 2.662 (9) Å apart) in [Na·C211·NCS].

In the solid state Na⁺ in [Na·C21C₅·NCS]⁺ and [Na·C211·NCS]⁺, respectively, has six and seven ligand donor atoms within bonding distance (Table II), and it is anticipated that Na⁺ will be at least six- and seven-coordinated in these cryptates in solution where NMR studies show the exclusive configuration is substantially retained.^{9–11} While in solution it is probable that some very labile contact ion pairing occurs between NCS⁻ (or ClO₄⁻ by which it is replaced in this study) and Na⁺ bound in the cryptates, the number of such contact sites and the ability of anions to compete with solvent for them is uncertain, and hence no indication of the occupancy of these sites is shown in the formulas [Na·C21C₅]⁺ and [Na·C211]⁺ employed below in discussions of the solution data. It has previously been shown that the ⁷Li chemical shift of inclusive [Li·C211]⁺ is invariant as the nature of the solvent is varied consistent with there being no significant contact between the completely encapsulated Li⁺ in [Li·C211]⁺ and the solvent.⁴ In contrast it is seen that the ²³Na chemical shift of exclusive [Na·C21C₅]⁺ varies by 3.70 ppm when the

solvent is changed from dimethylformamide to pyridine (Table I) consistent with the binding of one or more solvent molecules to Na⁺ in the cryptate. This shift variation is smaller than that observed for solvated Na⁺ (4.94 ppm) which is expected as bonding to the N₂O₃ ring of C21C₅ decreases the Na⁺ interaction with the solvent.

The kinetic parameters for the decomplexation of [Na·C21C₅]⁺ according to eq 1 are shown in Table III. These parameters are derived from the temperature variation of the mean lifetime of [Na·C21C₅]⁺, τ_c , determined by ²³Na NMR through eq 2 in which



$$k_d = 1/\tau_c = (k_B T/h) \exp(-\Delta H_d^*/RT + \Delta S_d^*/R) \quad (2)$$

all symbols have their usual meaning. The τ_c values ($\tau_c/P_c = \tau_s/P_s$, where τ is a lifetime P is a mole fraction, and the subscripts c and s refer to Na⁺ in the cryptate and solvated states, respectively) were derived through complete line shape analysis¹⁶ of the coalescing ²³Na resonances observed for solutions i–xii (Table I) as exemplified by Figure 1 in which the experimental and best fit calculated line shapes are shown for a selection of temperatures. (In dimethyl sulfoxide the Na⁺ exchange process was still in the fast exchange limit at 292 K, just above the melting point, at 79.39 MHz.)

In Figure 2 it is seen that the temperature variation of τ_c for each of the two solutions studied for a given solvent are indistinguishable (consistent with the predominant decomplexation path for [Na·C21C₅]⁺ being unimolecular) and that the magnitude of τ_c exhibits a marked dependence on the nature of the solvent. This is reflected, in the 1500-fold variation in k_d and the variations in the other kinetic parameters of Table III which are derived from the combined data for each pair of solutions studied for each solvent. This indicates a substantial involvement of the solvent in the rate-determining step leading to decomplexation. A lesser sensitivity to the nature of the solvent is shown by k_f which exhibits only a 44-fold variation. The formation process is envisaged to proceed through a diffusion-controlled encounter between Na⁺ and C21C₅ followed by a sequential partial desolvation of Na⁺ and formation of bonds to the N₂O₃ ring of C21C₅ to produce exclusive [Na·C21C₅]⁺, in which one or more solvent molecules remain bound to Na⁺. The decomplexation process is the reverse of this sequence of events. Before discussing the role of the solvent in the reaction mechanism it is appropriate to compare the kinetic data characterizing [Na·C211]⁺ and [Na·C21C₅]⁺. It is seen from Table III that k_d for [Na·C21C₅]⁺ is greater than k_d for [Na·C211]⁺ by factors of 538, 720, and 2380 in propylene carbonate, methanol, and dimethylformamide, respectively. This demonstrates the importance of the disruption of the bonding between

(17) Shannon, R. D. *Acta Crystallogr., Sect. A: Cryst. Phys., Diffraction, Gen. Crystallog.* 1976, A32, 751–767.

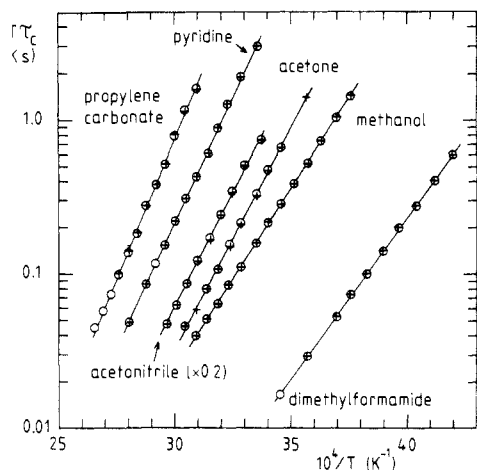


Figure 2. The temperature variation of $T\tau_c$ for Na^+ exchange on $[\text{Na}\cdot\text{C}21\text{C}_5]^+$ in a range of solvents. Circles and crosses represent datum points obtained from the solutions with the higher and lower total concentrations of $\text{C}21\text{C}_5$, respectively, listed in Table I for each solvent. The solid curves represent the best fit linear regression lines obtained for the simultaneous fit of each pair of data sets to the Eyring equation.

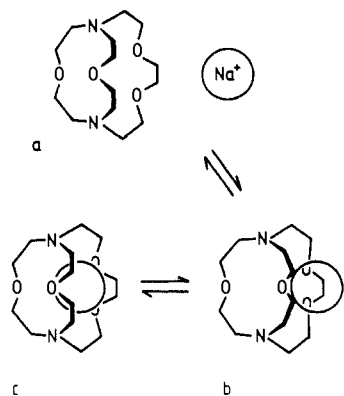


Figure 3. Proposed mechanism for Na^+ exchange on $[\text{Na}\cdot\text{C}211]^+$. The rate-determining step for decomplexation is considered to be that proceeding from exclusive $[\text{Na}\cdot\text{C}211]^+$ c to species b in which Na^+ is still bound to the O_3 face. One or more resolution steps then occur to produce solvated Na^+ and the free cryptand a.

Na^+ and the fourth oxygen of $[\text{Na}\cdot\text{C}211]^+$ opposite the N_2O_3 ring in the rate-determining step characterized by k_d , and the absence of this oxygen accounts for the greater lability of $[\text{Na}\cdot\text{C}21\text{C}_5]^+$ in the decomplexation process. Thus for $[\text{Na}\cdot\text{C}211]^+$ it is envisaged that k_d characterizes the disruption of the Na^+ interaction with the fourth oxygen which occurs synchronously with partial resolution of Na^+ and conformational change in $\text{C}211$. By analogy to the solid-state structures¹¹ it is anticipated that this step involves conformational changes in $\text{C}211$ and the outward movement of Na^+ by ca. 0.23 Å to a position ca. 0.37 Å from the O_3 plane similar to that observed for Na^+ in $[\text{Na}\cdot\text{C}21\text{C}_5]^+$ from which the fourth oxygen is absent (Table II). The release of Na^+ from the O_3 plane and the resolution of Na^+ then follows through a sequence of faster steps. (A simple representation of this mechanism in which no solvent is shown appears in Figure 3.) The interaction of Na^+ with the N_2O_3 ring in the ground state of $[\text{Na}\cdot\text{C}21\text{C}_5]^+$ is envisaged as being structurally similar to that existing in $[\text{Na}\cdot\text{C}211]^+$ after the first and rate-determining decomplexation step has occurred as shown in b in Figure 3. Thus the first step in the decomplexation of $[\text{Na}\cdot\text{C}21\text{C}_5]^+$ starts from a similar structure to that from which the second step starts for $[\text{Na}\cdot\text{C}211]^+$.

It is now appropriate to consider the role of the solvent in the formation and decomplexation of $[\text{Na}\cdot\text{C}21\text{C}_5]^+$. The free energies of solvated Na^+ , $\text{C}21\text{C}_5$, $[\text{Na}\cdot\text{C}21\text{C}_5]^+$, and the transition states will be determined to a substantial extent by the electron-donating ability of the solvent (as indicated by the Gutmann donor number

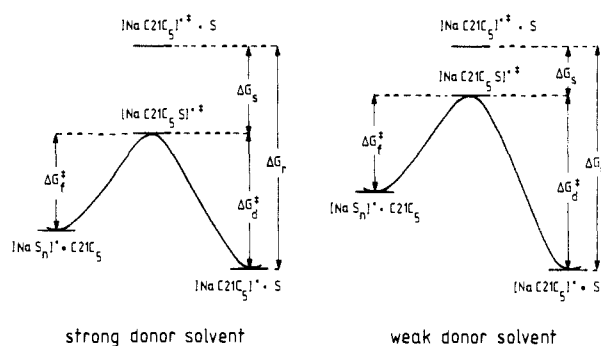


Figure 4. Simplified reaction profiles for the formation and decomplexation of $[\text{Na}\cdot\text{C}21\text{C}_5]^+$ in solvents in which k_f and k_d , respectively, show little and substantial variation with the nature of the solvent (S). The free energies of the $[\text{Na}\cdot\text{C}21\text{C}_5]^+ + \text{S}$ ground states in strong and weak donor solvents are normalized to the same value in both profiles. The solvent molecule shown bound in the transition-state $[\text{Na}\cdot\text{C}21\text{C}_5\text{S}]^+ \ddagger$ is in addition to those already bound in the $[\text{Na}\cdot\text{C}21\text{C}_5]^+$ ground states. The transition-state $[\text{Na}\cdot\text{C}21\text{C}_5]^+ \ddagger$ only exists in the absence of solvent participation in the activation process. The $[\text{Na}\cdot\text{S}_N]^+$ species represent the ground-state solvated ions. As a consequence of the uncertainty of the number of solvent molecules bound in each of the species shown in the profiles no attempt is made to balance the number of interacting solvent molecules along the reaction coordinate.

D_N^{18}), the number of solvent molecules bound to Na^+ in the fully solvated state and in $[\text{Na}\cdot\text{C}21\text{C}_5]^+$, the steric interactions of solvent molecules in these environments, and to a lesser extent, the secondary solvation of Na^+ , $\text{C}21\text{C}_5$, and $[\text{Na}\cdot\text{C}21\text{C}_5]^+$. Precise separation of these individual factors is not possible, but a trend is noticeable in the data of Table III. In acetonitrile, acetone, methanol, and dimethylformamide, k_f shows only a small sensitivity to the nature of the solvent, whereas k_d increases by several orders of magnitude as D_N increases. (Propylene carbonate and in particular pyridine deviate from this pattern as is discussed later.) This variation in k_d may be explained on the basis that ΔG_d^\ddagger for decomplexation is largely the difference between the free energy change arising from structural rearrangements in $[\text{Na}\cdot\text{C}21\text{C}_5]^+$ to achieve its transition-state stereochemistry in the absence of solvent interaction, ΔG_f^\ddagger , and the involvement of solvent in the activation process, ΔG_s^\ddagger , which causes an increased solvation of Na^+ in the $[\text{Na}\cdot\text{C}21\text{C}_5\text{S}]^+ \ddagger$ transition state. As the magnitude of ΔG_f^\ddagger is defined to be independent of solvent, ΔG_d^\ddagger will decrease as ΔG_s^\ddagger increases with the electron-donating power of the solvent as shown qualitatively in Figure 4. The free energy of activation of formation, ΔG_f^\ddagger , is shown as an invariant quantity in Figure 4 to represent qualitatively the relatively small dependence of k_f on the nature of the solvent which is discussed below.

In acetonitrile, acetone, methanol, and dimethylformamide k_d increases with D_N whilst ΔH_d^\ddagger decreases, and in each case ΔS_d^\ddagger is negative. By comparison the k_d observed in propylene carbonate and in particular in pyridine is considerably smaller than expected on the basis of D_N alone, the ΔH_d^\ddagger are correspondingly increased, and the ΔS_d^\ddagger are positive. Thus for the latter two solvents the tendency for k_d to increase with increase in D_N is apparently decreased by the steric hindrance arising from their ring structures, particularly in the case of pyridine where the N donor atom is within the ring structure. Overall it emerges that the transition state is stabilized with respect to ground-state $[\text{Na}\cdot\text{C}21\text{C}_5]^+$ to the greatest extent by those solvents with both the larger D_N and a stereochemistry which allows the close approach of the solvent donor atoms to Na^+ in the cryptate. (There is no obvious correlation of the variation of k_d with the variation of the solvent dielectric constant (Table III).) This implies that while bond breaking makes a major contribution to the k_d activation process, ΔG_d^\ddagger may be considerably decreased through synchronous resolution by a solvent such as dimethylformamide. This is in accord with the previously noted decrease in ΔH_d^\ddagger which infers

(18) Gutmann, V. *Coordination Chemistry in Nonaqueous Solutions*; Springer-Verlag: Wien, 1968.

an increased importance in bond making in the activation process and the negative ΔS_d^\ddagger values associated with the lower ΔH_d^\ddagger indicating an ordering in the transition state consistent with the binding of additional solvent molecules in the transition state. It is only in dimethylformamide that activation data are available for the decomplexation of both $[\text{Na}\cdot\text{C}_{21}\text{C}_5]^+$ and $[\text{Na}\cdot\text{C}_{211}]^+$ (Table III). The latter cryptate is characterized by a much greater ΔH_d^\ddagger and a substantial and positive ΔS_d^\ddagger which contrasts with the negative ΔS_d^\ddagger characterizing $[\text{Na}\cdot\text{C}_{21}\text{C}_5]^+$. This is consistent with the mechanistic proposals developed above in which bond breaking is more important in the decomplexation activation process starting from ground-state c in Figure 3 for $[\text{Na}\cdot\text{C}_{211}]^+$ than in the activation process for $[\text{Na}\cdot\text{C}_{21}\text{C}_5]^+$, probably because Na^+ is more accessible to solvent in the latter case. (The k_d values characterizing $[\text{Na}\cdot\text{C}_{21}\text{C}_5]^+$ and $[\text{Na}\cdot\text{C}_{211}]^+$ are substantially greater than the k_d value characterizing the inclusive cryptate $[\text{Na}\cdot\text{C}_{221}]^+$ (Table III) consistent with the rate-determining step for the decomplexation of the latter species involving a change from the inclusive to the exclusive form.)

In acetonitrile, acetone, methanol, and dimethylformamide, k_f characterizing $[\text{Na}\cdot\text{C}_{21}\text{C}_5]^+$ varies by a factor of 2.55 only which shows that the summation of the free energy changes accompanying the partial desolvation of Na^+ and the formation of Na^+ to C_{21}C_5 bonds in the activation process are similar. In propylene

carbonate and pyridine k_f is decreased which infers that the contributions to ΔG_f^\ddagger arising from the desolvation of Na^+ (and possibly solvation changes of C_{21}C_5) in these solvents are substantially greater than in the other four solvents. Thus propylene carbonate and pyridine in particular produce k_f and k_d values which are unexpected on the basis of the trends in these parameters observed for the other solvents studied. There are insufficient data available to ascertain if these kinetic differences induced by propylene carbonate and pyridine are general in cryptate systems, but the observation⁵ of $10^3 k_d(298.2 \text{ K}) = 0.13$ and 13.0 s^{-1} in pyridine and dimethylformamide, respectively, for the $[\text{Li}\cdot\text{C}_{211}]^+$ system indicates that pyridine produces small k_d values in one other cryptate system at least.

Acknowledgment. The award of a Commonwealth Postgraduate Research Award to I.M.B. and partial support from the Australian Research Grants Scheme is gratefully acknowledged.

Registry No. C_{21}C_5 , 72640-82-5; $[\text{Na}\cdot\text{C}_{21}\text{C}_5]^+$, 104911-16-2; Na , 7440-23-5.

Supplementary Material Available: Tables of experimental k_d ($= 1/\tau_c$) and experimental temperatures plotted in Figure 2 and corresponding to solutions i-xii of Table I (4 pages). Ordering information is given on any current masthead page.

Interaction between Lithium and Carbon Monoxide. 1. A Matrix Infrared Study

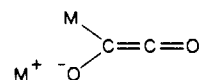
O. Ayed, A. Loutellier, L. Manceron, and J. P. Perchard*

Contribution from the Laboratoire de Spectrochimie Moléculaire, Université Pierre et Marie Curie, 75320 Paris Cédex 05, France. Received October 15, 1985

Abstract: Codeposition of lithium atoms and carbon monoxide molecules in an inert medium (Krypton) at 12 K led to the spontaneous formation of numerous products classified in three groups. The first group is constituted by four mononuclear species $\text{Li}(\text{CO})_n$ with $n = 1, 2, 3$, and ≥ 4 . In these cases, structures, vibrational spectra, and bonding have been discussed with the help of isotopic substitutions ($^6\text{Li}/^7\text{Li}$, $^{12}\text{C}/^{13}\text{C}$, $^{16}\text{O}/^{18}\text{O}$). The structural properties of the well-identified monolithium species are closely related to carbonyls of transition metals, but with stronger perturbations with Li for equal coordination numbers. The second group involves species with several Li atoms and one or two CO molecules in which the carbonyl groups are only weakly coupled in spite of larger perturbations than with mononuclear species. The third group corresponds to species identified by stretching modes of either CO single bonds or strongly coupled double bonds therefore species in which true chemical bonds are formed between carbonyls.

The state of knowledge of the carbonyl chemistry of alkali metals has remained up to now astonishingly low compared to that relating to transition metals. The reaction between alkali atoms (M) dissolved in liquid ammonia and carbon monoxide was reported for the first time in 1933 by Pearson¹ for $\text{M} = \text{Li}$. After evaporation of ammonia, a white solid with one-to-one stoichiometry was isolated with the following properties: it is stable at room temperature and decomposes at about 500 °C, with formation of Li_2CO_3 , Li_2O , and C; it reacts vigorously with water, with formation of Li_2CO_3 , C, and H_2 . More recently the structure of the reaction product for $\text{M} = \text{K}$ has been determined by X-ray crystallography.² The product has been shown to be potassium acetylenediolate ($\text{KOC}\equiv\text{COK}$) with the following internuclear distances (Å): K-O, 2.67; C-O, 1.28; C-C, 1.21.

Also evidence has been presented³ suggesting that in liquid ammonia another compound with the structure



is formed along with the acetylenediolate salt. On the other hand, some infrared spectra were reported for Li-CO complexes trapped in inert matrices by Margrave and co-workers.⁴ But to our knowledge, no detailed analysis of these data has been subsequently published.

This lack of interest in alkali metal carbonyls from the chemists and physicochemists (no specific publication on this topic since 1963) is probably due to the absence of applications of these carbonyls in preparative chemistry. However, the nature of the interaction between alkali metal atoms and carbon monoxide could be of major interest in catalysis, since it has been recognized⁵ that the catalytic properties of transition metal surfaces are modified

(1) Pearson, T. G. *Nature (London)* 1933, 131, 166.

(2) Weiss, E.; Büchner, W. *Helv. Chim. Acta* 1963, 46, 1121; *Z. Anorg. Allg. Chem.* 1964, 330, 251.

(3) Büchner, W. *Helv. Chim. Acta* 1963, 46, 2111.

(4) Ozin, G. A.; Moskovits, M. In *Cryochemistry*; Wiley: New York, 1976; p 345.

(5) Dry, M. E.; Shingles, T.; Boshoff, L. J.; Oosthuizen, G. J. *J. Catal.* 1969, 15, 190. See also: Broden, G.; Gafner, G.; Bonzel, H. P. *Surf. Sci.* 1979, 84, 295.